

# H3K27 acetylation activated-long non-coding RNA CCAT1 affects cell proliferation and migration by regulating SPRY4 and HOXB13 expression in esophageal squamous cell carcinoma

Erbao Zhang<sup>1,†</sup>, Liang Han<sup>2,†</sup>, Dandan Yin<sup>3,†</sup>, Xuezhi He<sup>1</sup>, Linzhi Hong<sup>4</sup>, Xinxin Si<sup>1</sup>, Mantang Qiu<sup>5</sup>, Tongpeng Xu<sup>4</sup>, Wei De<sup>1,\*</sup>, Lin Xu<sup>5,\*</sup>, Yongqian Shu<sup>4,\*</sup> and Jinfei Chen<sup>4,6,7,\*</sup>

<sup>1</sup>Department of Biochemistry and Molecular Biology, Nanjing Medical University, Nanjing, Jiangsu, PR China, <sup>2</sup>Department of Oncology, Xuzhou Central Hospital, Affiliated Xuzhou Hospital, College of Medicine, Southeast University, Xuzhou, Jiangsu, PR China, <sup>3</sup>Central laboratory, Second Affiliated Hospital of Southeast University, Nanjing, Jiangsu, PR China, <sup>4</sup>Department of Oncology, First Affiliated Hospital of Nanjing Medical University, Nanjing, Jiangsu, PR China, <sup>5</sup>Department of Thoracic Surgery, Jiangsu Key Laboratory of Molecular and Translational Cancer Research, Nanjing Medical University Affiliated Cancer Hospital, Cancer Institute of Jiangsu Province, Baiziting 42, Nanjing 210009, China, <sup>6</sup>Department of Oncology, Nanjing First Hospital, Nanjing Medical University, Nanjing, Jiangsu, PR China and <sup>7</sup>Collaborative Innovation Center for Cancer Personalized Medicine, Nanjing Medical University, Nanjing, Jiangsu, PR China

Received November 09, 2016; Editorial Decision November 24, 2016; Accepted November 29, 2016

## ABSTRACT

Recently, long non-coding RNAs (lncRNAs) have been shown to have important regulatory roles in human cancer biology. In our study, we found that lncRNA CCAT1, whose expression is significantly increased and is correlated with outcomes in Esophageal Squamous Cell Carcinoma (ESCC). Consecutive experiments confirmed that H3K27-acetylation could activate expression of colon cancer associated transcript-1 (CCAT1). Further experiments revealed that CCAT1 knockdown significantly repressed the proliferation and migration both *in vitro* and *in vivo*. RNA-seq analysis revealed that CCAT1 knockdown preferentially affected genes that are linked to cell proliferation, cell migration and cell adhesion. Mechanistic investigations found that CCAT1 could serve as a scaffold for two distinct epigenetic modification complexes (5' domain of CCAT1 binding Polycomb Repressive Complex 2 (PRC2) while 3' domain of CCAT1 binding SUV39H1) and modulate the histone methylation of promoter of SPRY4 (sprouty RTK signaling antagonist 4) in nucleus. In cytoplasm, CCAT1 regulates HOXB13 as a

molecular decoy for miR-7, a microRNA that targets both CCAT1 and HOXB13, thus facilitating cell growth and migration. Together, our data demonstrated the important roles of CCAT1 in ESCC oncogenesis and might serve as targets for ESCC diagnosis and therapy.

## INTRODUCTION

With variable geographic distribution, esophageal cancer represents the sixth leading cause of cancer mortality and the eighth most common type of cancer worldwide (1,2). There are two common types of esophageal cancer: esophageal adenocarcinoma (EAC) and esophageal squamous cell carcinoma (ESCC). Although EAC is increasing rapidly in Western countries, ESCC is increasing at the fastest rate of all cancers in East Asian (3). Due to diagnosis is rarely made prior to advanced disease stages, the overall 5-year survival rate remains extremely poor (4). Therefore, a better understanding of the molecular mechanisms underlying ESCC progression will supply an arm for improving the diagnosis and treatment of human ESCC.

With development of whole-genome sequencing technology, it was determined that protein-coding sequences occupy less than 2% of the human genome (5). Long non-

\*To whom correspondence should be addressed. Tel: +86 025 8686 2728; Fax: +86 025 8686 2728; Email: dewei\_njmu@sina.com  
Correspondence may also be addressed to Lin Xu. Tel: +86 025 83284700; Fax: +86 025 83641062; Email: xulin\_njmu@163.com  
Correspondence may also be addressed to Yongqian Shu. Tel: +86 025 6813 6428; Fax: +86 025 8372 4440; Email: nanjingyongqianshu@163.com  
Correspondence may also be addressed to Jinfei Chen. Tel: +86 025 87726234; Fax: +86 025 87726234; Email: jinfeichen\_edu@126.com

†These authors contributed equally to this work as the first authors.

coding RNAs (lncRNAs) are a class of transcripts longer than 200 nucleotides with limited protein coding potential (6). Recently, more and more studies have shown that lncRNAs could play critical roles in many biological processes including cellular development, differentiation, etc (7–11). In addition, the aberrant expressions of lncRNAs have been shown in various types of cancers, including ESCC (12–19). Many studies revealed that lncRNAs could play an important role in regulating gene expression at different levels, including chromatin modification, transcriptional and post-transcriptional processing (20,21). For instance, HO-TAIR could involve in transcriptional repression of HOX loci and promote breast metastasis by binding to the PRC2 (polycomb repressive complex 2) (12). In addition to regulation of transcription levels, lncRNAs could also serve as a ‘sponge’ to titrate microRNAs, thus participating in post-transcriptional processing (10,22).

Colon cancer associated transcript-1 (CCAT1), was firstly identified by Nissan *et al.* and was highly expressed in CRC but not in normal tissues (23). Moreover, CCAT1 have exhibited oncogenic property in various type of cancer, including hepatocellular carcinoma, gallbladder cancer and gastric cancer (24–26). However, the exact molecular mechanism and global genes that were mediated by CCAT1 remains unclear. And the biological functions of CCAT1 in the control of ESCC tumorigenesis have not been well characterized. These prompted us to explore the role of CCAT1 in human ESCC.

In our present study, we found that H3K27 acetylation could activate CCAT1 and CCAT1 was significantly upregulated in ESCC tissues compared with the corresponding non-tumor tissues and may serve as an independent predictor for the overall survival in ESCC. In addition, CCAT1 could regulate cell proliferation and migration both *in vitro* and *in vivo*. RNA-seq analysis revealed that CCAT1 knock-down preferentially affected genes that are linked to proliferation and migration-related genes. Mechanistic investigations found that CCAT1 could exhibit different regulatory mechanisms in nucleus and cytoplasm, thus regulating SPRY4 and HOXB13 expression and affecting cell proliferation and migration in ESCC.

## MATERIALS AND METHODS

### Tissue collection and Ethics statement

A total of 90 patients analyzed in this study underwent resection of the ESCC at the First Affiliated Hospital of Nanjing Medical University. The study was approved by the Ethics Committee of Nanjing Medical University (Nanjing, Jiangsu, PR China), and it was performed in compliance with the Declaration of Helsinki Principles. And written informed consent was obtained from all patients. The clinicopathological characteristics of the ESCC patients are summarized in Table 1.

### RNA extraction and qRT-PCR analyses

Total RNA was extracted from tissues or cultured cells using TRIzol reagent (Invitrogen, Carlsbad, CA, USA). For qRT-PCR, RNA was reverse transcribed to cDNA by using a Reverse Transcription Kit (Takara, Dalian, China).

Real-time PCR analyses were performed with SYBR Green (Takara, Dalian China). Results were normalized to the expression of  $\beta$ -actin. The rest of primers were listed in Supplementary Table S1.

### Cell culture

ESCC cell lines Eca-109 and TE-1 were purchased from the Institute of Biochemistry and Cell Biology of the Chinese Academy of Sciences (Shanghai, China). Cells were cultured in DMEM (GIBCO-BRL) medium supplemented with 10% fetal bovine serum (FBS), 100 U/ml penicillin and 100 mg/ml streptomycin in humidified air at 37°C with 5% CO<sub>2</sub>.

### Plasmid constructs

CCAT1 and SPRY4 cDNA was synthesized and cloned into the expression vector pcDNA3.1 (Invitrogen). The CCAT1 fragments for RNA pull down assays were then used as a template for generating constructs carrying deletions using respective primers. All PCR products were verified by DNA sequencing.

### Transfection of cell lines

The siRNAs and plasmid were transfected into ESCC cells using Lipofectamine2000 (Invitrogen) according to the manufacturer’s instructions. Scrambled negative control siRNA (si-NC) were purchased from Invitrogen (Invitrogen, CA, USA). All the sequences for siRNAs and shRNA were listed in Supplementary Table S1. Interference target sequence of EZH2 and SUV39H1 were acquired according to previous study (33,55). The HOXB13 siRNA was from Santa Cruz (sc-43851). The shCCAT1 (AAGCAGGCAGAAAGCCGUAUCUAAA) was cloned into pENTR™/U6 vector.

LNA-ASO targeting CCAT1 and negative control LNA-ASO were designed and synthesized by Exiqon (Exiqon, Vedbaek, Denmark). ESCC cells were transfected with the LNA-ASOs at the final concentration of 100 nM using Oligofectamine transfection reagent (Invitrogen) according to the manufacturer’s instructions. Cells were harvested for analyses 48 h after transfections. The sequences of ASO were listed in Supplementary Table S1.

### Cell proliferation analysis

Cell viability was tested with MTT kit (Sigma) according to the manufacturer’s instruction. For colony formation assay, a certain number of transfected cells were placed in each well of 6-well plates and maintained in proper media containing 10% FBS for two weeks, during which the medium was replaced every 4 days. Colonies were then fixed with methanol and stained with 0.1% crystal violet (Sigma) in PBS for 15 min. Colony formation was determined by counting the number of stained colonies. BrdU experiments were performed using a BrdU Cell Proliferation Assay Kit (Millipore, Cat.No.2750) according to the manufacturer’s instructions. The higher OD reading represents the higher BrdU concentration in the sample.

**Table 1.** The clinic-pathological factors of 90 ESCC patients

Characteristics	Expression of CCAT1		P-value*
	Low	High	
Sex			0.832
Male	24	25	
Female	21	20	
Age			0.398
≤60	23	19	
>60	22	26	
Histological grade			0.29
Low	22	27	
Middle or high	23	18	
Tumor invasion depth (T)			0.203
T1/T2	23	17	
T3/T4	22	28	
Lymph node metastasis (N)			0.035*
N0	26	16	
N1	19	29	
TNM stage			0.003*
I/II	30	16	
III/IV	15	29	

\*chi-square test.

\* $P < 0.05$ .

### Cell migration assays

For the migration assays, after transfection,  $5 \times 10^4$  cells in serum-free media were placed into the upper chamber of an insert (8- $\mu\text{m}$  pore size; Millipore, Billerica, MA, USA). Medium containing 10% FBS was added to the lower chamber. After incubation for 24 h, the cells remaining on the upper membrane were removed with cotton wool. Cells that had migrated through the membrane were stained with methanol and 0.1% crystal violet, imaged and counted using an IX71 inverted microscope (Olympus, Tokyo, Japan). Experiments were independently repeated three times.

### Western blot assay and antibodies

Cells protein lysates were separated by 10% sodium dodecyl sulphate-polyacrylamide gel electrophoresis (SDS-PAGE) transferred to 0.22  $\mu\text{m}$  NC membranes (Sigma) and incubated with specific antibodies. Autoradiograms were quantified by densitometry (Quantity One software; Bio-Rad).  $\beta$ -actin antibody was used as control. Anti-EZH2, Anti-SUV39H1, Anti-SPRY4 and Anti-HOXB13 was from Abcam (Hong Kong, China).

### In vivo assay

Athymic male mice were purchased from the Animal Center of the Chinese Academy of Science (Shanghai, China) and maintained in laminar flow cabinets under specific pathogen-free conditions. For cell proliferation assay *in vivo*, Eca-109 cells were stably transfected with shRNA and empty vector and harvested from cell culture plates, then cells were xenografted into BALB/c male nude mice. The tumor volumes and weights were measured every 2 days in mice; the tumor volumes were measured as length  $\times$  width<sup>2</sup>  $\times$  0.5. Sixteen days after injection, the mice were killed and tumor weights were measured and used for further analysis.

Eca-109 cells were stably transfected with shRNA and empty vector and harvested from cell culture plates, washed

with PBS and re-suspended at  $2 \times 10^7$  cells/ml. Suspended cells (0.1 ml) were injected into the tail veins of nine mice, which were sacrificed 7 weeks after injection. The lungs were removed and photographed, and visible tumors on the lung surface were counted. This study was carried out in strict accordance with the Guide for the Care and Use of Laboratory Animals of the National Institutes of Health. Our protocol was approved by the Committee on the Ethics of Animal Experiments of Nanjing Medical University.

### Subcellular fractionation location

The separation of the nuclear and cytosolic fractions was performed using the PARIS Kit (Life Technologies, Carlsbad, CA, USA) according to the manufacturer's instructions.

### Chromatin immunoprecipitation assays

Chromatin immunoprecipitation (ChIP) assays were performed using EZ-CHIP KIT according to the manufacturer instruction (Millipore, USA). EZH2 and SUV39H1 were obtained from Abcam. H3 trimethyl Lys 27 antibody, Histone H3 and Acetyl-Histone H3 Lys27 was from Millipore. The ChIP primer sequences were listed in Supplementary Table S1. Quantification of immunoprecipitated DNA was performed using qPCR. ChIP data were calculated as a percentage relative to the input DNA by the equation  $2^{[\text{Input Ct} - \text{Target Ct}]} \times 0.1 \times 100$ .

### Whole transcriptome deep sequencing

Total RNA from the Eca-109 cells with CCAT1 knockdown and control Eca-109 cells were isolated and quantified. The concentration of each sample was measured by NanoDrop 2000 (Thermo Scientific, USA). The quality was assessed by the Agilent2200 (Agilent, USA). The sequencing library

of each RNA sample was prepared by using Ion Proton Total RNA-Seq Kit v2 according to the protocol provided by manufacturer (Life technologies, USA). Data are available in Supplementary Table S2 (six samples).

### RNA immunoprecipitation assays

RNA immunoprecipitation (RIP) experiments were performed using a Magna RIP™ RNA-Binding Protein Immunoprecipitation Kit (Millipore, USA) according to the manufacturer's instructions. Antibody for RIP assays of EZH2, SUZ12, DNMT1, DNMT3a, DNMT3b, WDR5, LSD1, SETDB1 and SUV39H1 were from Abcam.

### In vitro Transcription Assays and RNA pull down assays

*In vitro* Translation Assays were performed using Mmessage Mmachine KIT according to the manufacturer instruction (Ambion, USA). Then CCAT1 RNAs were labeled by Desthiobiotinylation by using Pierce RNA 3' End Desthiobiotinylation Kit (Pierce, Thermo). Then RNA pull down assays were performed by Pierce Magnetic RNA-Protein Pull-Down Kit according to the manufacturer instruction (Pierce, Thermo).

### Co-immunoprecipitation and Western blotting

Cell pellet was resuspended in Buffer A (10 mM Hepes pH7.5, 1.5 mM MgCl<sub>2</sub>, 10 mM KCl, 0.5 mM DTT and 1 mM PMSF/Cocktail) for 10 min on ice, 0.25% NP-40 was added for 5 min and Cytosol fraction and nuclear pellets were obtained by centrifugation at 13 000 RPM for 10 min. Nuclear pellet was then resuspended in Buffer C (20 mM Hepes pH 7.5, 10% Glycerol, 0.42 M KCl, 4 mM MgCl<sub>2</sub>, 0.2 mM EDTA, 0.5 mM DTT and 1 mM PMSF/cocktail) 20 min on ice and Nuclear fraction was obtained after 13 000 RPM 10 min centrifugation. Cytosol fraction and Nuclear fraction were mixed together and 500 μg of lysate was used for one IP reaction. Antibodies were added and IP was performed on the rotating plate in 4°C for 3 h, and 20 μl washed A/G beads (Pierce) were added and incubated for 1 h. Quickly wash four times with Wash buffer (50 mM TrisCl 7.9, 10% Glycerol, 100 mM KCl, 0.2 mM EDTA, 5 mM MgCl<sub>2</sub>, 10 mM β-ME 0.1% NP-40). Precipitates were purified and analysed by Western blotting by standard procedures using indicated antibodies at a dilution of 1:500.

### Bioinformatics analyses

Bioinformatics were used to predict this possibility of interaction of CCAT1 and a panel of methylation modifiers (histone methylation and DNA methylation), including EZH2, SUZ12, WDR5, LSD1, SETDB1, SUV39H1, DNMT1, DNMT3a and DNMT3b. Predictions with probabilities > 0.5 were considered positive. RPISeq predictions are based on random forest or support vector machine. The online URL: (<http://pridb.gdcb.iastate.edu/RPISeq/references.php>).

### Luciferase reporter assay

To construct luciferase reporter vectors, HOXB13 3'-UTR and CCAT1 cDNA fragment containing the predicted micro-RNAs binding sites were amplified by PCR, and then subcloned downstream of the luciferase gene in the pGL3 plasmid. Mutant of plasmids (pGL3-HOXB13-3'UTR-MUT and pGL3-CCAT1-MUT) were generated by site directed mutagenesis PCR reaction using platinum pfx DNA polymerase following the product manual. All constructs were verified by DNA sequencing. The luciferase assays were performed using a luciferase assay kit (Promega, Madison, WI, USA) according to the manufacturer's protocol. Briefly, cells were first transfected with appropriate plasmids in 24-well plates. Next, the cells were collected and lysed for luciferase assay 48 h after transfection. The relative luciferase activity was normalized with renilla luciferase activity.

### Statistical analysis

All statistical analyses were performed using SPSS 20.0 software (IBM, SPSS, USA). The significance of differences between groups was estimated by Student's *t*-test,  $\chi^2$  test or Wilcoxon test, as appropriate. Overall survival rates were calculated by the Kaplan–Meier method with the log-rank test applied for comparison. Survival data were evaluated using univariate and multivariate Cox proportional hazards model. Variables with a value of  $P < 0.05$  in univariate analysis were used in subsequent multivariate analysis on the basis of Cox regression analyses. Two-sided  $P$ -values were calculated, and a probability level of 0.05 was chosen for statistical significance.

## RESULTS

### H3K27 acetylation activated-CCAT1 is upregulated in human ESCC tissues and correlates with poor prognosis

The level of CCAT1 was detected in 90 paired ESCC tissues and adjacent normal tissues by qRT-PCR, and normalized to  $\beta$ -actin. As shown in Figure 1A, CCAT1 expression was significantly up-regulated in 80.7% (79 of 90 paired) ESCC tissues ( $9.9048 \pm 14.56661$ ,  $P < 0.001$ ). Next, we explored the correlation between CCAT1 expression and the clinic-pathological factors of patients with ESCC. In general, CCAT1 level was associated with lymph node metastasis and TNM stage. Patients with advanced TNM stage (III/IV) or positive lymph node metastasis were associated with higher CCAT1 expression, whereas patients with local TNM stage (I/II) or negative lymph node metastasis were associated with lower CCAT1 level ( $14.0684 \pm 18.73862$  versus  $5.9221 \pm 7.13882$ ,  $P = 0.009$  and  $12.9935 \pm 18.29238$  versus  $6.3748 \pm 7.28609$ ,  $P = 0.024$ ) (Figure 1B and C). Furthermore, we divided the samples into high (above the mean,  $n = 45$ ) and low (below the mean,  $n = 45$ ) CCAT1 expression groups according to the median value of CCAT1 levels. Chi-square test was performed to evaluated clinic-pathological factors between the two groups. As shown in Table 1, CCAT1 level was also correlated to lymph node metastasis ( $P = 0.035$ ) and TNM stage ( $P = 0.003$ ). Other clinic factors such as histological grade, tumor invasion depth, patients' sex and age were found not to

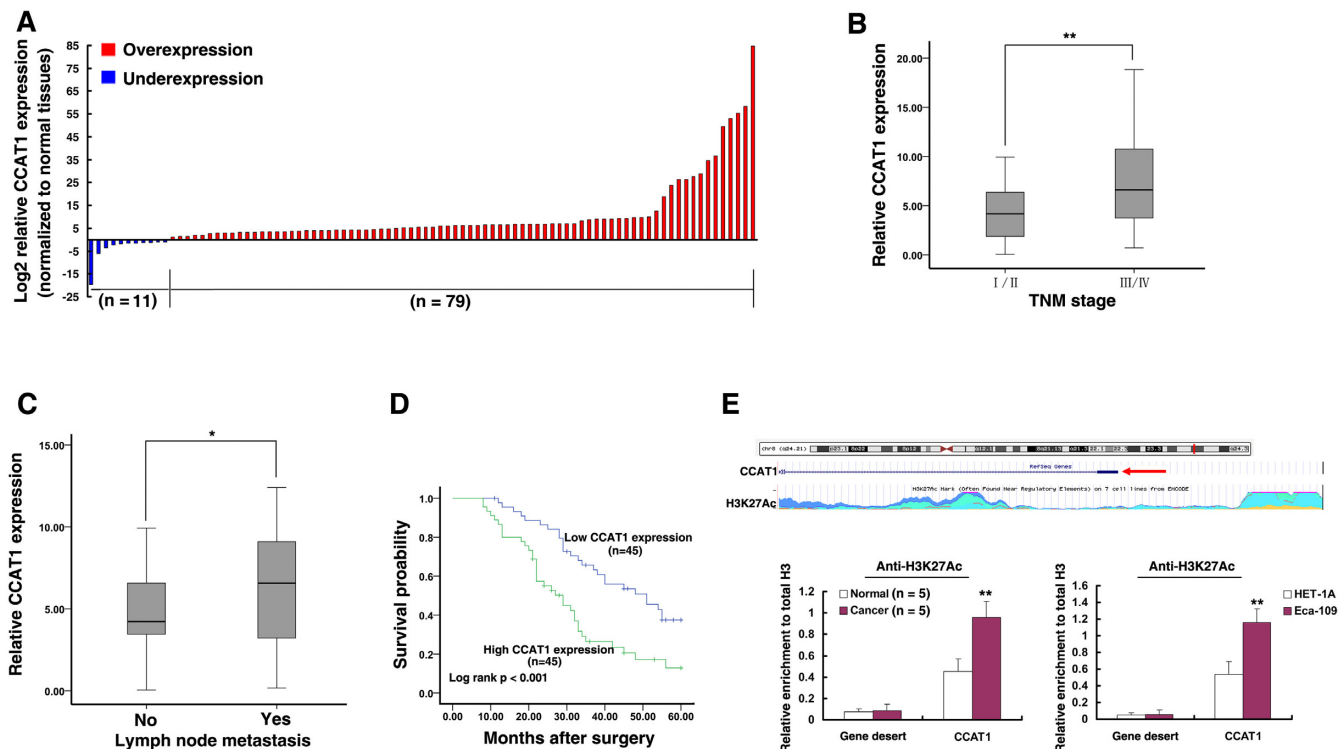


**Figure 1.** Expression of colon cancer associated transcript-1 (CCAT1) in esophageal squamous cell carcinoma (ESCC) tissues and its clinical parameters and H3K27 acetylation could activate CCAT1 in ESCC. (A) CCAT1 was detected in 90 pairs of ESCC tissues by qRT-PCR. The levels of CCAT1 in ESCC tissues are significantly higher than those in non-tumorous tissues. (B and C) CCAT1 expression was significantly higher in patients with an advanced TNM stage and positive lymph node metastasis. (D) Patients with high levels of CCAT1 expression showed reduced survival times compared with patients with low levels of CCAT1 expression ( $P < 0.001$ , log-rank test). (E) UCSC Genome Bioinformatics Site (<http://genome.ucsc.edu/>) showed high enrichment of H3K27Ac at the promoter of CCAT1. ChIP assays detected the H3K27Ac acetylation at promoter of CCAT1 in ESCC tissues and cells. \* $P < 0.05$ , \*\* $P < 0.01$ .

be significantly associated with CCAT1 expression in this study.

To determine the relationship between CCAT1 expression and ESCC patients' prognosis, we attempted to evaluate the correlation between CCAT1 expression and clinical outcomes. Kaplan–Meier analysis and log-rank test were used to evaluate the effects of CCAT1 expression and the clinicopathological characteristics on overall survival. The median survival time for low CCAT1 expression groups was  $44.162 \pm 2.442$  months, while that for high CCAT1 expression groups was only  $30.646 \pm 2.507$  months. As shown in Figure 1D, overexpression of CCAT1 predicted a poor prognosis in patients with ESCC ( $P < 0.001$ ).

To further confirm the prognostic role of CCAT1 in ESCC patients, the univariate and multivariate survival analysis (Cox proportional hazards regression model) were performed. Univariate analysis identified six prognostic factors: TNM stage, histological grade, distant metastasis, tumor invasion depth, lymph node metastasis and CCAT1 expression. Multivariate analysis further revealed that CCAT1 expression could be regarded as an independent predictor for overall survival in patients with ESCC ( $P < 0.001$ ), as well as TNM stage ( $P = 0.015$ ) and histological grade ( $P = 0.008$ ) (Table 2).

To explore the mechanism of high expression of CCAT1 in ESCC, firstly, by using UCSC Genome Bioinformatics Site (<http://genome.ucsc.edu/>), we found high enrichment of

H3K27Ac at the promoter of CCAT1. By ChIP assays, we found gain of H3K27Ac in cancer tissues compared with normal tissues ( $n = 5$ ) at the promoter of CCAT1. And we also found gain of H3K27Ac in ESCC cells (Eca-109) compared with normal human esophageal epithelial cells (HET-1A) at the promoter of CCAT1 (Figure 1E). Taken together, these data confirm that CCAT1 is frequently increased in ESCC, histone acetylation activation of promoter may partly account for this dysregulation.

### CCAT1 regulates ESCC cell proliferation and migration *in-vitro*

To explore the role of CCAT1 in ESCC, firstly, as shown in Supplementary Figure S1A, the siRNA-mediated knock-down and plasmid-mediated overexpression were used for exogenously manipulating expression of CCAT1, both in Eca-109 and TE-1 cell lines. Then MTT assays showed that knockdown of CCAT1 expression significantly inhibited cell proliferation compared with the control cells. In contrast, overexpressed CCAT1 could promote cell proliferation (Figure 2A). Similarly, the result of colony-formation assay revealed that clonogenic survival was significantly decreased following knockdown of CCAT1. And overexpression of CCAT1 could boost the number of clones (Figure 2B). Then BrdU assays demonstrated that CCAT1 had a significant impact on ESCC cell proliferation (Figure 2C).

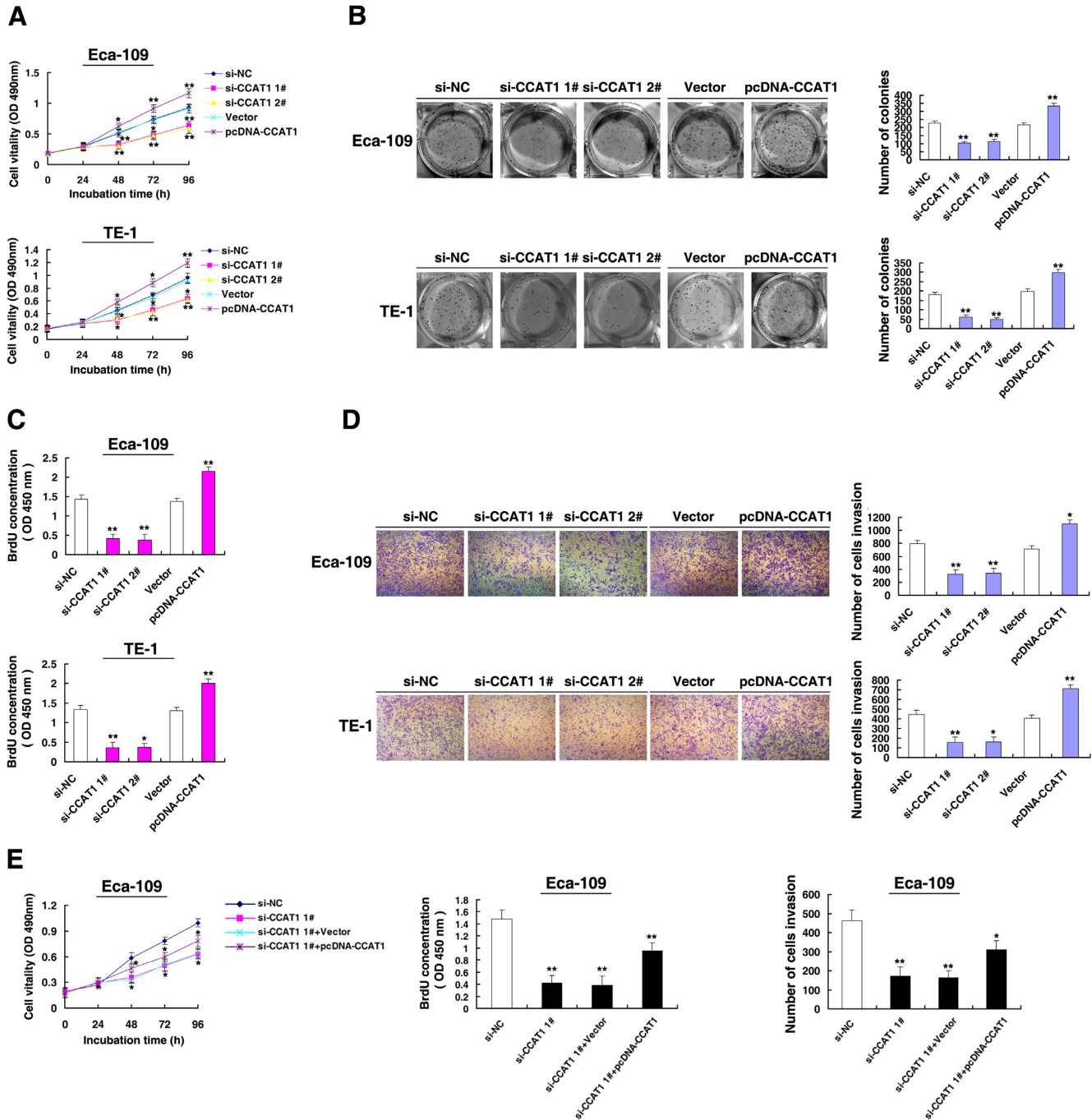


**Figure 2.** CCAT1 regulates ESCC cell proliferation and migration *in vitro*. (A) MTT assays were performed to determine cell proliferation of Eca-109 and TE-1 cells after transfection of overexpression plasmid and si-RNA of CCAT1. (B) Representative results of colony formation of Eca-109 and TE-1 cells transfected with overexpression plasmid and si-RNA of CCAT1. (C) BrdU assays were used to detect the cell proliferation after transfection, respectively. (D) Transwell assays were used to investigate the changes in migratory abilities of ESCC cells after transfection, respectively. (E) Eca-109 cells transfected with si-NC/si-CCAT1 and transfected with si-CCAT1 followed by transfection with pcDNA-CCAT1. After transfection, cells were analyzed by MTT, BrdU and Transwell assays. \* $P < 0.05$ , \*\* $P < 0.01$ .

**Table 2.** Univariate and multivariate analysis of clinic pathologic factors for overall survival in 90 patients with ESCC

Risk factors	Univariate analysis			Multivariate analysis		
	HR <sup>a</sup>	P-value	95% CI	HR	P-value	95% CI
CCAT1 expression	1.053	<0.001**	1.034~1.072	1.044	<0.001**	1.023~1.066
TNM stage (I/II/, III/IV)	5.134	<0.001**	2.949~8.941	3.622	0.015*	1.279~10.253
Histological grade (low, middle or high)	2.085	0.006**	1.240~3.508	2.143	0.008**	1.215~3.780
Distant metastasis (Yes, No)	8.956	<0.001**	3.468~23.130	2.655	0.078	0.897~7.860
Tumor invasion depth(T1/T2, T3/T4)	3.564	<0.001**	2.040~6.225	1.961	0.156	0.773~4.977
Lymph node metastasis (N0, N1)	1.756	0.030*	1.055~2.923	0.0.769	0.406	0.414~1.428
Age ( $\leq 60$ , $> 60$ )	1.173	0.538	0.706~1.950			
Sex (male, female)	1.357	0.249	0.808~2.279			

HR hazard ratio.

\*P &lt; 0.05.

\*\*P &lt; 0.01.

Next, transwell assays revealed that knockdown of CCAT1 significantly repressed cell migration compared with the control cells. In contrast, overexpression of CCAT1 could promote cell migration (Figure 2D). To further confirm the function of CCAT1, rescue experiment found that overexpression of CCAT1 could significantly reverse CCAT1 knockdown-mediated growth and migration suppression (Figure 2E).

#### CCAT1 regulates ESCC cell proliferation and migration *in vivo*

To further determine whether the CCAT1 affects tumorigenesis of ESCC *in vivo*, Eca-109 cells stably transfected with sh-CCAT1 or control vector were inoculated into nude mice. Sixteen days after the injection, the tumors formed in the sh-CCAT1 group were substantially smaller than those in the control group (Figure 3A and B). Moreover, the mean tumor weight at the end of the experiment was markedly lower in the sh-CCAT1 group compared with control vector group (Figure 3C). Tumors formed from stably sh-CCAT1-transfected Eca-109 cells exhibited decreased positivity for Ki-67 than those from control cells (Figure 3D). These findings indicate that knockdown of CCAT1 inhibits tumor growth *in vivo*.

To validate the effects of CCAT1 on the metastasis of Eca-109 cells *in vivo*, Eca-109 cells stably transfected with sh-CCAT1 or control vector were injected into the tail veins of nine mice. Metastatic nodules on the surface of the lungs were counted after 7 weeks. Ectopic knockdown of CCAT1 reduced the number of metastatic nodules compared with the control group (Figure 3E). This difference was further confirmed following examination of the entire lungs, and through hematoxylin and eosin (H&E) staining of lung sections (Figure 3E). Our *in vivo* data therefore complemented the results of functional *in vitro* studies involving CCAT1.

#### CCAT1 serves as modular scaffold for EZH2 and SUV39H1 in nucleus, thus epigenetically silencing of SPRY4

To probe the CCAT1-associated pathway on an unbiased basis in ESCC, we assessed the gene expression profiles of Eca-109 cells that were suppressed for CCAT1. We performed RNA transcriptome sequencing from control or siRNAs against CCAT1. A common set of 828 mRNAs showed  $\geq 1.5$ -fold increased abundance and silencing CCAT1 also reduced the abundance ( $\leq 1.5$ -fold) of 553 genes (Figure 4A, Supplementary Table S2). Gene ontol-

ogy analysis showed that the most significantly overrepresented biological processes included pathways involved in cell proliferation, cell migration and cell adhesion, as well as cell apoptosis (Figure 4B). These included many well-known proliferation and migration-related genes (e.g. HPGD, ADAM19, CASP14, IGFBP1, FAT4, SPRY4, KLF6, BTG2, IGFBP3, GDF15, FAS, p15, p27, COX17, ATF4, JUND, HOXB13, CDC25B, CCND3, MMP14, MMP28, MAPK4 and AQP8 et al). To further confirm the function of CCAT1, we also designed LNA-ASO targeting CCAT1 and control LNA-ASO. QPCR studies confirmed that transfection with CCAT1-ASO efficiently reduced CCAT1 expression in Eca-109 and TE-1 cells (Supplementary Figure S1B). These genes were selectively confirmed by qRT-PCR after knockdown and overexpression of CCAT1 in Eca-109 and TE-1 cells (Figure 4C and D).

Recent studies have reported that a significant number of lncRNAs have been shown to function in cooperation with chromatin modifying enzymes to promote epigenetic activation or silencing of gene expression (27). Especially, PRC2, a methyltransferase, which is composed of EZH2, SUZ12 and EED, can catalyze the di- and trimethylation of lysine residue 27 of histone 3 (H3K27me3), thus epigenetically modulating gene expression (28). Previous study found that  $\approx 20\%$  of all human lncRNAs have been shown to physically associate with PRC2, suggesting that lncRNAs may have a general role in recruiting polycomb-group proteins to their target genes (29). To explore the mechanism for CCAT1-mediated regulation, firstly, subcellular fractionation location assays demonstrated the localization of CCAT1 to both in the nucleus and cytoplasm (Figure 5A). Then through bioinformatics analysis showed positive possibility for a panel of chromatin modifiers, including WDR5 (H3K4me3), LSD1 (H3K4me3), SETDB1 (H3K9me3), SUV39H1 (H3K9me3), DNMT1, DNMT3a, DNMT3b, EZH2 (H3K27me3) and SUZ12 (H3K27me3) (<http://pridb.gdcb.iastate.edu/RPISeq/references.php>) (Figure 5B). Then we employed RIP with a panel of antibodies. As shown in Figure 5B, in addition to PRC2, there was a substantial enrichment in RIPs of SUV39H1, U1 as negative control. Studies have showed that lncRNAs could act as scaffold for distinct protein complexes (30–32). SUV39H1 (Suppressor of variegation 3–9 homolog 1), a histone methyltransferase, catalyzes histone 3 lysine 9 trimethylation (33). And both EZH2 and SUV39H1 could show a property of oncoepigenic in tumorigenesis (34). Therefore we hypothesized that CCAT1 may coordinately interact with both

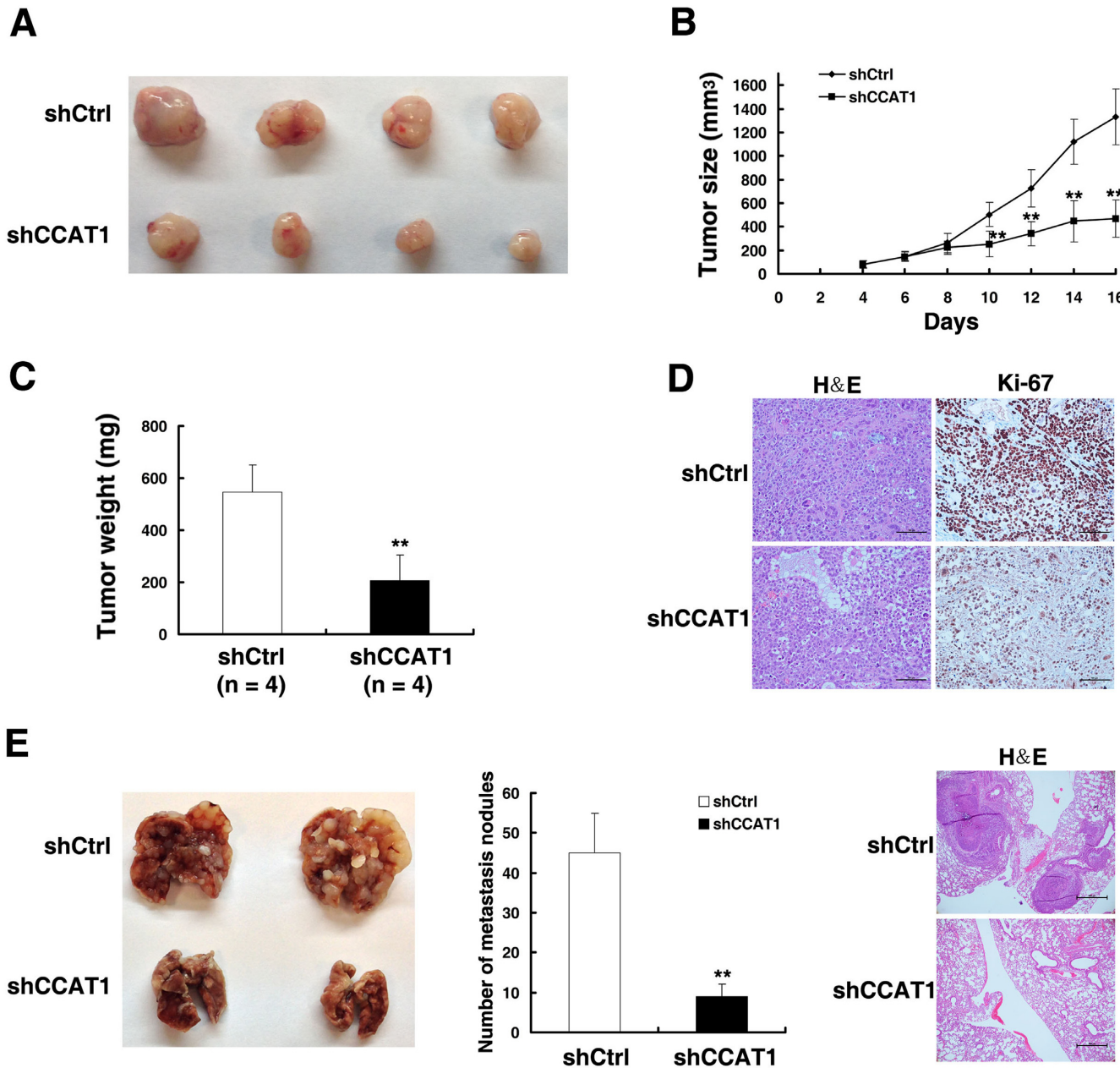


**Figure 3.** CCAT1 regulates ESCC cell proliferation and migration *in vivo*. (A and B) Scramble or shCCAT1 was stably transfected into Eca-109 cells, which were injected in the nude mice, respectively. Tumor volumes were calculated after injection every 2 days. Bars indicate S.D. (C) Tumor weights are represented as means of tumor weights  $\pm$  S.D (standard deviation). (D) Histopathology of xenograft tumors. The tumor sections were under H&E staining and IHC staining using antibodies against Ki-67. Bar, 100  $\mu$ m. Error bars indicate means  $\pm$  S.E.M (standard error of the mean). The size bar was indicated in the figure. (E) Analysis of an experimental metastatic animal model was performed by injecting Eca-109 cells stably transfected with CCAT1-knockdown into nude mice. Lungs from mice in each experimental group, with the numbers of tumor nodules on lung surfaces, are shown. Visualization of the entire lung and HE-stained lung sections. Bar, 100  $\mu$ m. The size bar was indicated in the figure. \* $P < 0.05$ , \*\* $P < 0.01$ .

PRC2 and SUV39H1. To test this, RNA pull down assays demonstrated that labeled CCAT1 RNA, but not empty vector or an antisense CCAT1, specifically retrieved EZH2 and SUV39H1 from Eca-109 cell nuclear extract (Figure 5C). Using a series of CCAT1 deletion mapping, the EZH2 binding activity mapped to nucleotides 1–600 of CCAT1, while the SUV39H1 binding activity mapped to nucleotides 2400–2795 (Figure 5C). The existence of independent binding sites for EZH2 and SUV39H1 on CCAT1 suggests that

CCAT1 may bridge EZH2 and SUV39H1. EZH2 IP retrieved SUV39H1, and SUV39H1 IP retrieved EZH2 in turn from Eca-109. Knockdown CCAT1 (ASO) of the IP abrogated the interaction between EZH2 and SUV39H1, suggesting that CCAT1 is required to bridge this interaction (Figure 5C). Then the role of EZH2/SUV39H1 in coregulating suppression of these CCAT1-suppressed genes was investigated by EZH2 and SUV39H1 knock-down (EZH2, the key catalytic subunit of PRC2 histone

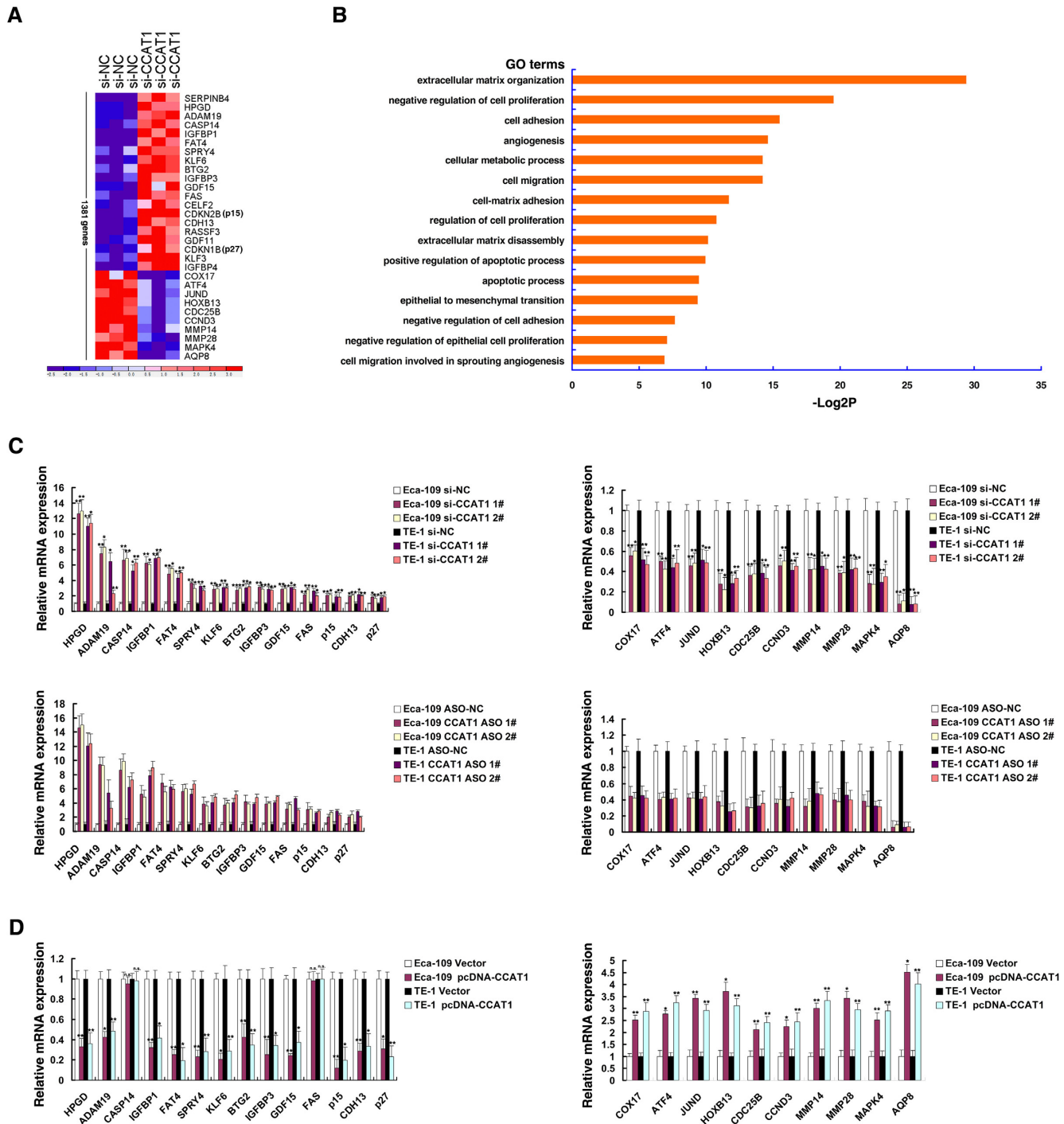


**Figure 4.** RNA-seq after CCAT1 knockdown in Eca-109 cells. **(A)** Mean-centered, hierarchical clustering of 828 transcripts altered ( $\geq 1.5$ -fold change) in si-NC-treated cells and siRNA-CCAT1-treated cells, with three repeats. **(B)** Gene ontology analysis for all genes with altered expressions. **(C and D)** The altered mRNA levels of genes were selectively confirmed by qRT-PCR in knockdown CCAT1 (siRNA and ASO) and overexpression of CCAT1. \* $P < 0.05$ , \*\* $P < 0.01$ . n.s., not significant.

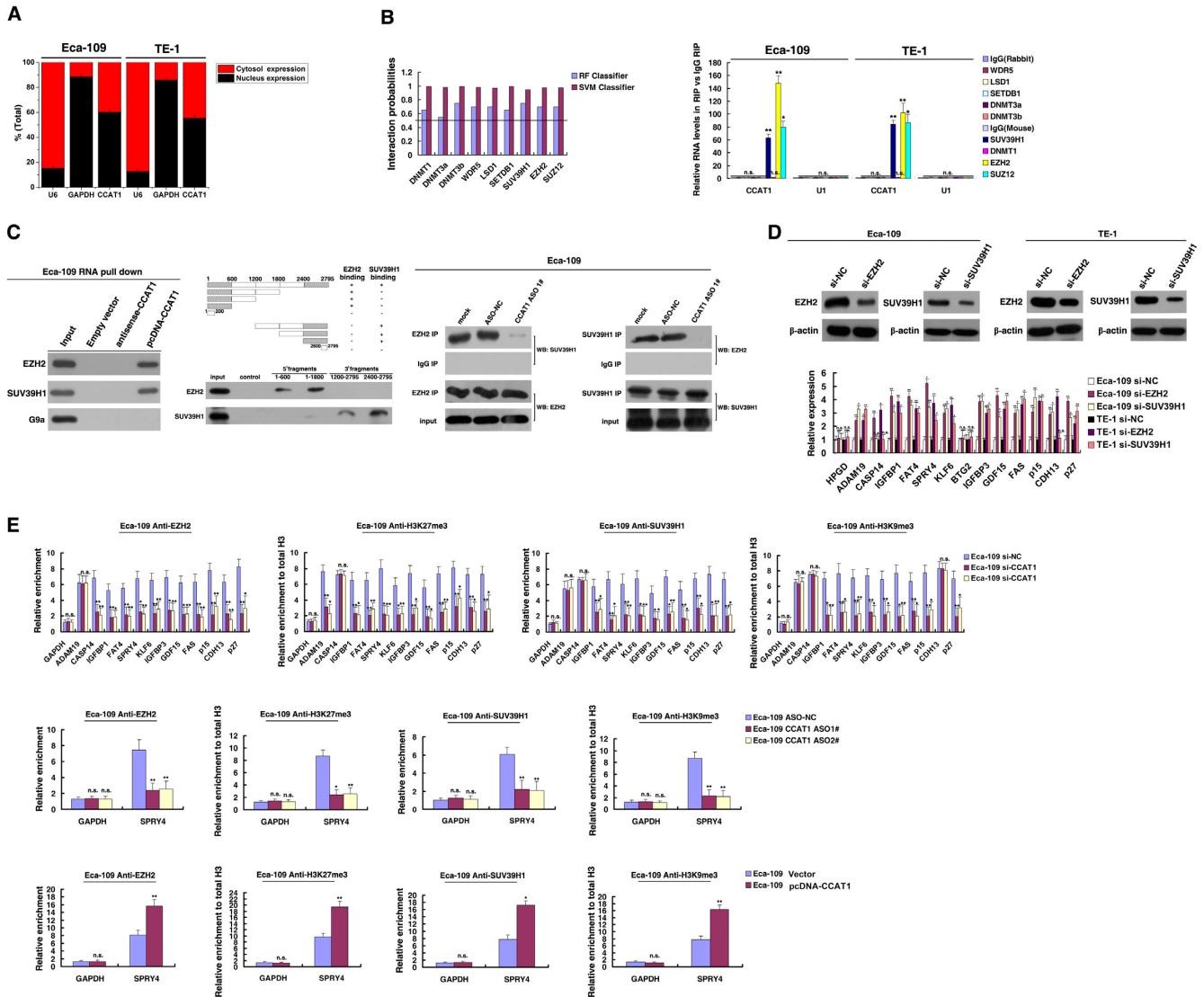


**Figure 5.** CCAT1 serves as modular scaffold of EZH2 and SUV39H1. (A) After nuclear and cytosolic separation, RNA expression levels were measured by qRT-PCR. GAPDH was used as a cytosol marker and U6 was used as a nucleus marker. (B) Bioinformatics were used to predict this possibility of interaction of CCAT1 and a panel of methylation modifiers (histone methylation and DNA methylation), including EZH2, SUZ12, WDR5, LSD1, SETDB1, SUV39H1, DNMT1, DNMT3a and DNMT3b. Predictions with probabilities > 0.5 were considered positive. RIPseq predictions are based on Random Forest (RF) or Support Vector Machine (SVM). RIPs experiments for EZH2/SUZ12/WDR5/LSD1/SETDB1/SUV39H1/DNMT1/DNMT3a and DNMT3b were performed and the coprecipitated RNA was subjected to qRT-PCR for CCAT1. (C) *In vitro* transcribed, pull down assays showed that desthiobiotinylation-CCAT1 could retrieve EZH2 and SUV39H1 in Eca-109 cells, but not G9a. G9a was a negative control. The first 600 bp of CCAT1 is necessary and sufficient to bind EZH2; the last 395 bp is necessary and sufficient to bind SUV39H1. The profiles are established by RNA pull-down of Eca-109 extract; retrieved proteins are detected by immunoblotting. In Eca-109 cells, EZH2 interacts with SUV39H1. Knockdown of CCAT1, but not si-NC, abrogates this interaction. (D) Western blot assays detected the expression of EZH2/ SUV39H1 after si-RNA transfection in Eca-109 and TE-1 cell lines. These methylation-related genes were detected by qPCR in Eca-109 and TE-1 cell lines, after knockdown EZH2 and SUV39H1. (E) ChIP-qPCR of EZH2/H3K27me3 and SUV39H1/H3K9me3 of the promoter region of these methylation-related genes locus after siRNA/ASO/plasmid treatment targeting CCAT1 in Eca-109 cells. Antibody enrichment was quantified relative to the amount of input DNA. Antibody directed against IgG was used as a negative control. \**P* < 0.05, \*\**P* < 0.01. n.s., not significant.

methyltransferase), and most were induced by knockdown of EZH2/SUV39H1 (Figure 5D). In addition, many studies have shown that these genes were affected by promoter hypermethylation in cancer. Then ChIP assays demonstrated that knockdown of CCAT1 decreased the binding of EZH2/SUV39H1 and H3K27me3/H3K9me3 levels across the promoters of the most coregulating genes (Figure 5E).

One of the coregulating genes, SPRY4, locating in 5q31 and encoding member of a family of cysteine- and proline-rich proteins, could inhibit cancer cell proliferation and migration, including breast cancer, prostate cancer and in non-small cell lung cancer (35–37). In addition, Hypermethylation of the SPRY4 promoter region has been reported to contribute to SPRY4 transcriptional inactivation (36,38). Our results found that knockdown of CCAT1

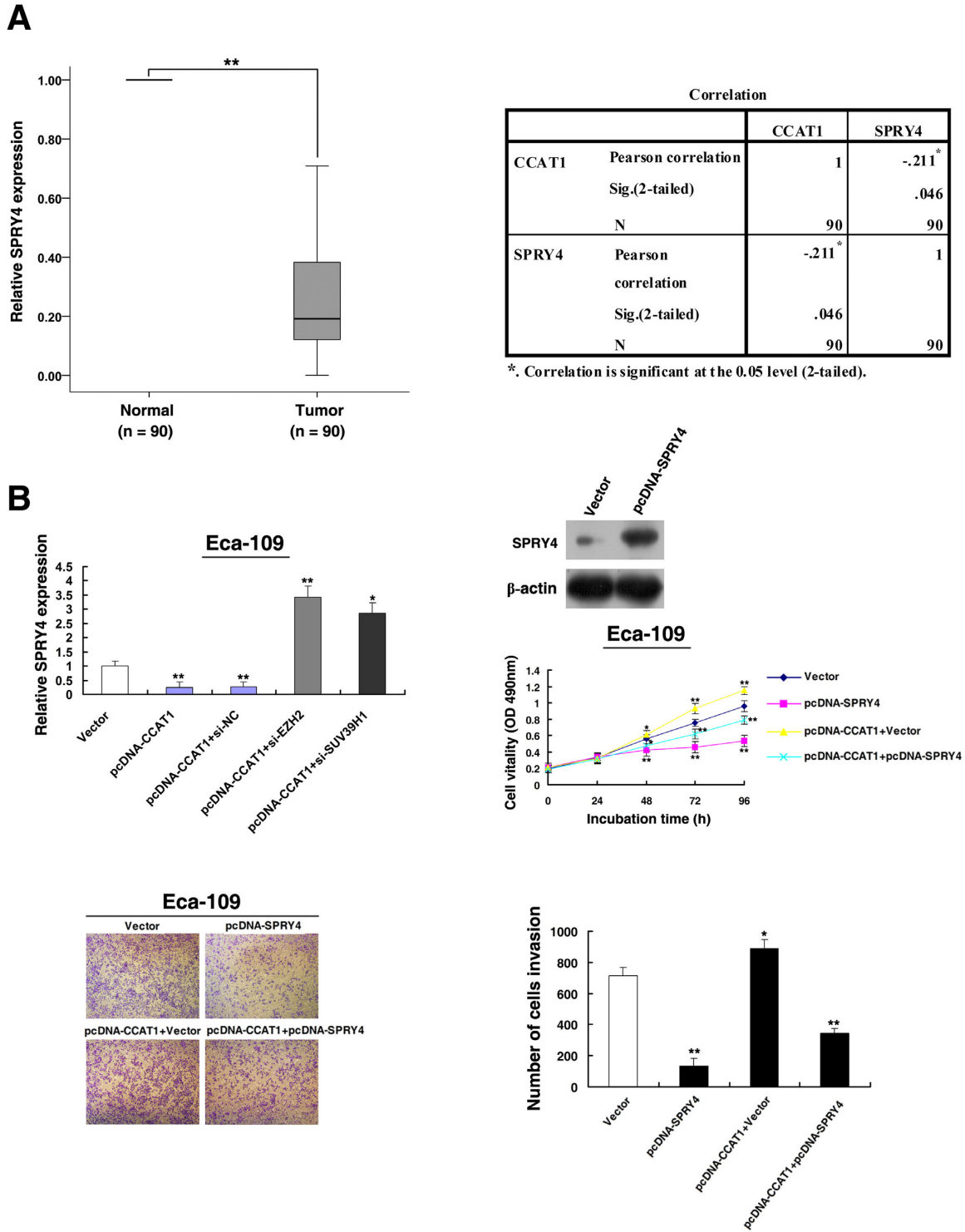


**Figure 6.** SPRY4 is a bona target of CCAT1 and SPRY4 over-expression suppresses ESCC cell proliferation and metastasis. (A) By qRT-PCR assays, the level of SPRY4 was obviously downregulated in 90 pairs ESCC tissues. The level of CCAT1 in ESCC tissues showed a statistically negative correlation with the relative level of SPRY4 expression (N = 90). (B) Relative expression was determined in CCAT1-overexpressing Eca-109 cells and cells simultaneously transfected with EZH2/SUV39H1 siRNA by qRT-PCR. Eca-109 cells transfected with Vector/SPRY4/pcDNA-CCAT1 and transfected with CCAT1 followed by transfection with SPRY4. After transfection, cells were analyzed by MTT assays and Transwell assays. \* $P < 0.05$ , \*\* $P < 0.01$ .

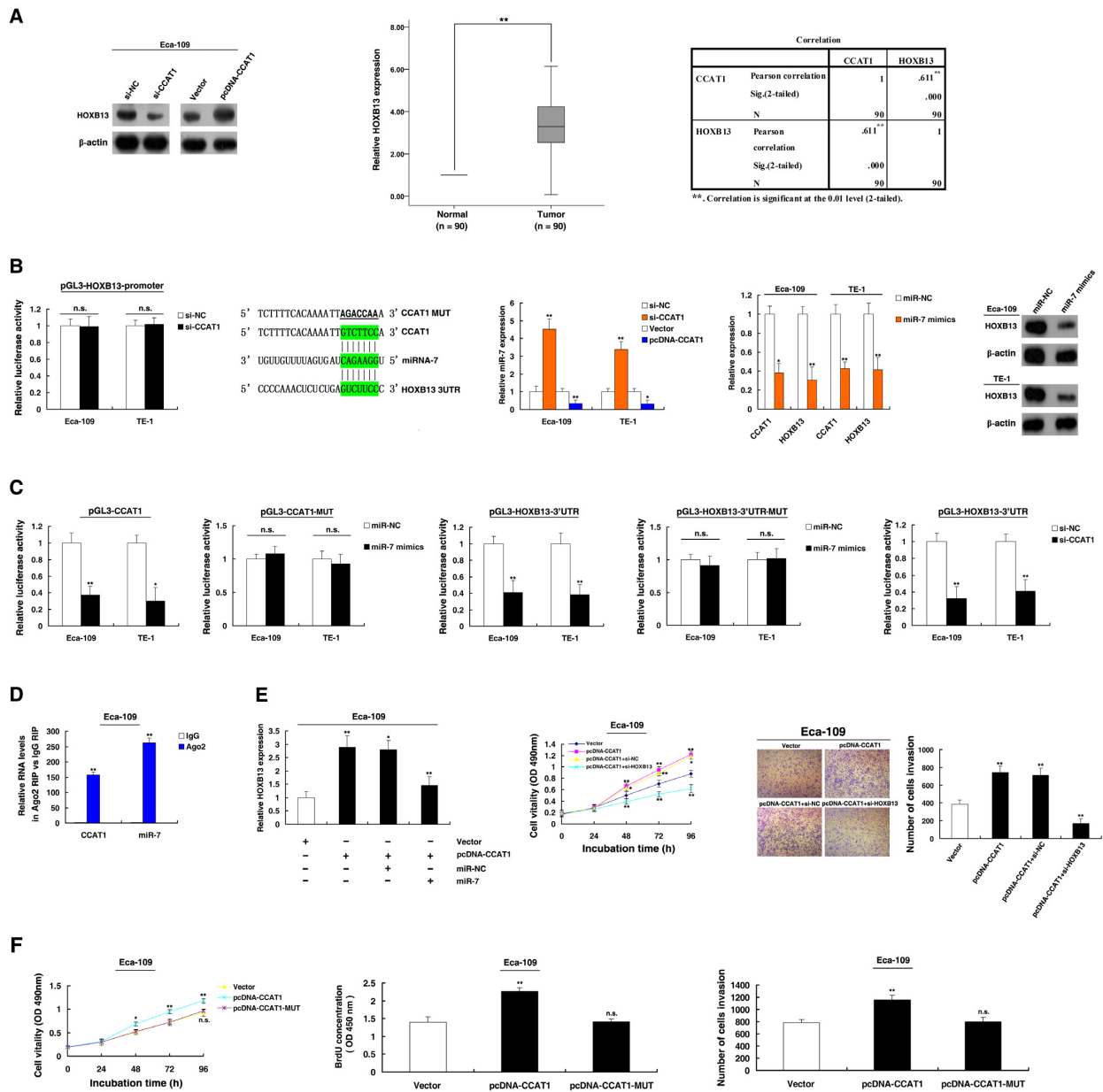


**Figure 7.** CCAT1 promotes HOXB13 expression by competing for miR-7 in cytoplasm, thus facilitating ESCC cell growth and migration. (A) Western blot assays detected the expression of HOXB13 after knockdown of CCAT1 and overexpression of CCAT1 in Eca-109 cells. qRT-PCR assays showed that the level of HOXB13 was obviously upregulated in 90 pairs ESCC tissues. The level of CCAT1 in ESCC tissues showed a statistically positive correlation with the relative level of HOXB13 expression (N = 90). (B) CCAT1 displays no effect on the transactivity of HOXB13 promoter. The promoter of HOXB13 was cloned upstream of a luciferase reporter gene, and the resultant construct was co-transfected with si-NC/si-CCAT1 in Eca-109 and TE-1 cells. The RNAup algorithm predicted potential binding of miR-7 to CCAT1 and to HOXB13, with considerable sequence complementary in the indicated regions. qRT-PCR assays detected the expression of miR-7 after knockdown of CCAT1 and overexpression of CCAT1 in Eca-109 and TE-1 cells. qRT-PCR assays detected the expression of CCAT1/HOXB13 after overexpression of miR-7 in Eca-109 and TE-1 cells. Western blot assays detected the expression of HOXB13 after knockdown of overexpression of miR-7 in Eca-109 and TE-1 cells. (C) Both CCAT1 and HOXB13 are targeted by miR-7. The 3'UTR of HOXB13 mRNA and full length of CCAT1 were respectively inserted downstream of a luciferase gene. The reporter vector was co-transfected with a renilla luciferase vector (for normalization) to Eca-109 and TE-1, which were treated by miR-7 mimics or control mimics. The luciferase signals of both reporter genes were significantly decreased when cells were treated with miR-7 mimics. Mutant 3'UTR of HOXB13 and CCAT1 is not affected by miR-7. The 3'UTR of HOXB13 and CCAT1 was mutated on the predicted binding site that is shown in (B), and was tested in the luciferase assay as described above. The results showed that miR-7 did not alter the luciferase signal. CCAT1 is required for the stability of HOXB13 3'UTR. The reporter vector was co-transfected with a renilla luciferase vector (for normalization) to Eca-109 and TE-1 cells, which were treated by CCAT1 siRNA or control siRNA. The luciferase signal of reporter gene was significantly decreased when knockdown of CCAT1. (D) RIPs experiments showed that CCAT1 was obviously enriched in Ago2-immunoprecipitation relative to control IgG. Similarly, miR-7 was also detected in Ago2-immunoprecipitation relative to control IgG control. Successful immunoprecipitation of Ago2-associated RNA was verified by qRT-PCR. (E) The promotion of HOXB13 by CCAT1 was significantly reversed by miR-7, by using qPCR assays. MTT and Transwell assays showed that knockdown HOXB13 could reverse CCAT1-mediated growth and migration promotion. (F) Eca-109 cells transfected with Vector/pcDNA-CCAT1 and pcDNA-CCAT1-Mutation. After transfection, cells were analyzed by MTT, BrdU and Transwell assays. \* $P < 0.05$ , \*\* $P < 0.01$ . n.s., not significant.

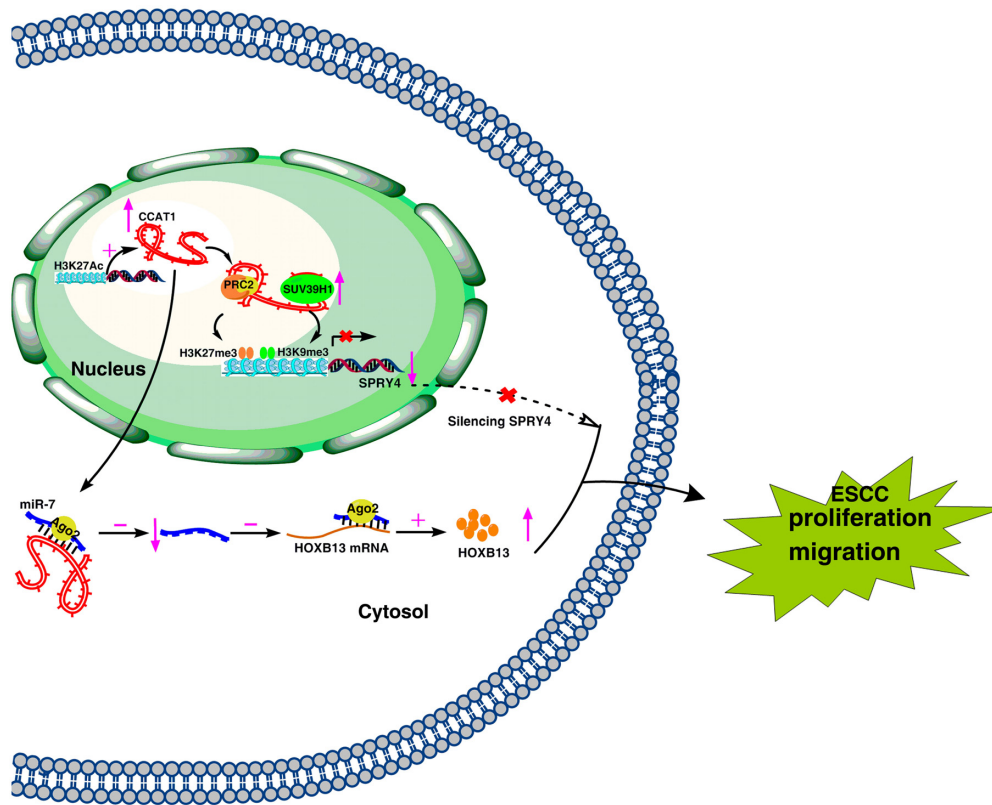


**Figure 8.** Proposed model which mediated by CCAT1 in proliferation and migration progression of ESCC.

by using ASO decreased the binding of EZH2/SUV39H1 and H3K27 trimethylation/H3K9 trimethylation levels across the promoters of SPRY4, and overexpression of CCAT1 could increase the binding of EZH2/SUV39H1 and H3K27 trimethylation/H3K9 trimethylation levels, confirming that SPRY4 was a bona target of CCAT1-regulated genes. In an attempt to understand the biological role of SPRY4 in ESCC, firstly, qRT-PCR analysis found that SPRY4 expression was significantly decreased in 90 pairs of ESCC tissues. Further analysis found that CCAT1 were negatively correlated with SPRY4 expression (Figure 6A). And the suppression of SPRY4 by CCAT1 was reversed when EZH2/SUV39H1 was simultaneously down-regulated (Figure 6B). Then overexpression of SPRY4 could significantly suppress Eca-109 proliferation and migration, and overexpression of SPRY4 could partly reverse CCAT1-mediated growth and migration promotion (Figure 6B). These results suggest that CCAT1 affects ESCC cell growth and migration at least partly through the epigenetic repression of SPRY4 by serving as modular scaffold for EZH2 and SUV39H1 in nucleus.

#### **CCAT1 promotes HOXB13 expression by competing for miR-7 in cytoplasm, thus facilitating ESCC cell proliferation and migration**

RNA-Seq found that knockdown of CCAT1 could obviously decrease a series of genes that promote proliferation and migration in ESCC. HOXB13, a member of HOX gene family, is one of the most commonly altered in solid tumors.

And HOXB13 could promote cancer cell proliferation and migration (39). We verified these results at protein level (Figure 7A). Moreover, qRT-PCR analysis found that HOXB13 was significantly upregulated in 90 pairs of ESCC tissues. Further analysis demonstrated that CCAT1 were positively correlated with HOXB13 expression (Figure 7A).

To probe the mechanism for CCAT1-regulated HOXB13 expression, we firstly tested whether CCAT1 could regulate the transactivation of HOXB13 mRNA. Luciferase assays demonstrated that CCAT1 did not impact the transactivation of HOXB13 promoter (Figure 7B), suggesting that CCAT1 may modulate HOXB13 mRNA after it is transcribed. Figure 5A found that CCAT1 were distributed both in the nucleus and cytoplasm, particularly those of the cytoplasmic form, are far from being elucidated. Recently, a new regulatory mechanism has been identified in which crosstalk between lncRNAs and mRNAs occurs by competing for shared microRNAs response elements (10). Interestingly, a microRNA, miR-7, was predicted to target both CCAT1 and HOXB13 (40) (Figure 7B). Further experiments found that knockdown CCAT1 increased miR-7 expression, and opposite results were found in CCAT1 overexpression. Moreover, treatment by miR-7 mimics significantly reduced CCAT1 and HOXB13 RNA and protein levels (Figure 7B).

To validate the effects of miR-7, we cloned the CCAT1, mutant CCAT1, 3'UTR of HOXB13 and mutant 3'UTR of HOXB13 downstream of diverse luciferase genes, and co-transfected these reporters with miR-7 mimics in Eca-109

and TE-1 cells. As expected, miR-7 significantly decreased the luciferase signals of reporters of CCAT1 and 3'UTR of HOXB13 (Figure 7C). However, miR-7 had no effect on mutant reporters of CCAT1 and 3'UTR of HOXB13 (Figure 7C). These results directly confirmed that miR-7 could target CCAT1 and HOXB13. Importantly, as a result, knockdown CCAT1 significantly reduced the luciferase intensity of 3'UTR of HOXB13, indicating that CCAT1 is required for the abundant expression of HOXB13 (Figure 7C).

miRNAs are known to be present in the cytoplasm in the form of miRNA ribonucleoprotein complexes that also contain Ago2, the core component of the RNA-induced silencing complex. To test whether CCAT1 associates with Ago2, RIP assays were performed on Eca-109 and TE-1 cell extracts using antibodies against Ago2. As shown in Figure 7D, CCAT1 and miR-7 were all obviously enriched in Ago2-immunoprecipitation relative to control IgG.

Furthermore, the promotion of HOXB13 by CCAT1 was reversed when treatment by miR-7 mimics (Figure 7E). Moreover, knockdown HOXB13 induced obviously proliferation and migration suppression in Eca-109 cells. In addition, knockdown HOXB13 could reverse CCAT1-mediated growth and migration promotion (Figure 7E and Supplementary Figure S1C). To further confirm the sequence site of function of CCAT1, we constructed a plasmid with a mutation of the mir7 target sequence in CCAT1. The mutation-related information was shown in Figure 7B. Then MTT, BrdU and transwell assays showed that mutant plasmid of CCAT1 could not promote cell growth and migration of ECSS cell (Figure 7F).

## DISCUSSION

To date, the newly discovered lncRNAs have emerged as an important player in cellular development and human diseases, especially in cancer. In our present study, we found that the level of CCAT1 in ESCC tissues was significantly higher than those in corresponding non-tumor tissues. The high expression of CCAT1 in ESCC patients was positively correlated with advanced TNM stage and positive lymph node metastasis. Moreover, high CCAT1 expression in ESCC tissues was associated with a poor prognosis and could be an independent prognostic indicator. These results suggested that CCAT1 might exhibit important role in ESCC progression. Previous studies found that CCAT1 was upregulated in breast cancer, hepatocellular carcinoma, gallbladder cancer, gastric cancer and colorectal cancer and could promote cancer cell proliferation and invasion (24–26,41,42). They also found that CCAT1 was a direct target of c-MYC (42,43). Although CCAT1 has been studied in different types of cancer, the possible role of CCAT1 in ESCC remains to be clarified. Our results revealed that H3K27Ac acetylation activation of promoter also partly contributed to upregulation of CCAT1 in ESCC. Similar to protein-coding transcripts, the transcription of lncRNAs is subject to typical epigenetics-mediated and transcription factor-mediated regulation. For instance, histone deacetylase3 Suppressed lncRNA-LET in hepatocellular carcinoma by reducing the histone acetylation-mediated modulation of promoter region (44). lncRNA MEG3 was

loss in tumor due to an increase in CpG methylation within the promoter (45). Our previous studies also found that EZH2 could epigenetically repress lncRNA SPRY4-IT1 in lung cancer and SP1 induce upregulation of lncRNA TINCR and E2F1 induce lncRNA ANRIL in gastric cancer and lung cancer (46–49).

In our study, we found that inhibition of CCAT1 could repress ESCC cell proliferation and migration both *in vitro* and *in vivo*. CCAT1 has exhibited oncogenic property in various types of cancer, however, the global genes that were affected by CCAT1 remains unclear. We found that knockdown CCAT1 induced inhibition of proliferation and migration ESCC cell line by RNA-Seq, and noting that results of gene ontology analysis was mainly proliferation and migration related. Recent studies have reported that a significant number of lncRNAs have been shown to function in cooperation with chromatin modifying enzymes to promote epigenetic activation or silencing of gene expression (27). Moreover, lncRNAs could act as scaffold for distinct protein complexes (30–32). Our results found that CCAT1 could serve as a scaffold for two distinct histone methylation modification complexes in nucleus, thus regulating a series of genes expression. In addition, many studies have shown that these genes were affected by promoter hypermethylation in cancer.

SPRY4 could exhibit function of tumor suppressor genes in various types of cancer. However, the role of SPRY4 in tumorigenesis of ESCC remains unclear. Moreover, previous studies have found that DNA methylation of the SPRY4 promoter region has been reported to contribute to SPRY4 transcriptional inactivation (36,38). Our results found that histone methylation (H3K9me3 and H3K9me3) mediated by CCAT1 could also contribute to the lower expression of SPRY4 in cancer. In addition, studies have showed that histone methylation usually cooperate with DNA methylation in heritable repression of gene activity (50,51). Our results demonstrated that CCAT1 serves as modular scaffold for EZH2 and SUV39H1, thus epigenetically silencing of SPRY4 in nucleus.

HOX genes are essential for morphogenesis and development (52). The dysregulation of HOX gene expression has been shown in many diverse cancers (53). As a member of the HOX gene family, high levels of HOXB13 promote tumorigenesis in different types of tumors. However, the mechanism of high expression of HOXB13 and the role of HOXB13 remains unclear. Here, we provide the evidence that the post-transcriptional regulation of HOXB13 is partly mediated by CCAT1 in tumor progression of ESCC, through competing for miR-7 in cytoplasm, thus facilitating ESCC cell proliferation and migration. And reduced levels of miR-7 have been linked to the development of cancer and metastasis (54). In addition, Ma *et al.* found that CCAT1 could promote gallbladder cancer development via 'sponging' miRNA-218-5p. These results proved that CCAT1 simultaneously sponge miR-7 and miR-218-5p. Cesana *et al.* found that linc-MD1 'sponges' miR-133 and miR-133 to regulate the expression of related genes in muscle differentiation (10).

In summary, CCAT1 promotes cell growth and migration through epigenetically regulating transcription of SPRY4 in nucleus. In cytoplasm, CCAT1 boosts proliferation and mi-

gration by competing for miR-7, thus facilitating cell survival and metastasis of ESCC. Our study found that CCAT1 could display different regulatory mechanisms in tumorigenesis of CCAT1. Our data may supply a strategy for targeting with the CCAT1 as a potential biomarker and a therapeutic target for patients with ESCC (Figure 8).

## SUPPLEMENTARY DATA

Supplementary Data are available at NAR Online.

## ACKNOWLEDGEMENTS

This work was partly supported by the Program for Development of Innovative Research Teams, by Jiangsu Province Clinical Science and Technology Projects (Clinical Research Center, BL2012008), National Natural Science Foundation of China (81172140, 81272532, 81401873 and 81502071) and the Priority Academic Program Development of Jiangsu Higher Education Institutions (JX10231801). And the work was also partly supported by the National 973 Basic Research Program of China (Grant No. 2013CB911300) grants from the National Natural Science Foundation of China (Grant No. 81272469 and 81572928) and the clinical special project for Natural Science Foundation of Jiangsu Province (Grant No. BL2012016), and the grant from Nanjing 12th Five-Year key Scientific Project of medicine to Dr Jinfei Chen.

*Author contributions:* E.-B.Z., L.H. and D.-D.Y. contributed to designing and organizing the experiments, carrying out the data analysis and writing of the manuscript. X.H., L.H., X.S., M.Q. and T.X. contributed to laboratory measurements, data analysis. W.D., L.X., Y.S. and J.C. contributed to conceiving the ideas, supervising the study and writing the manuscript.

## FUNDING

National Natural Science Foundation of China (81372321 and 81572261 to Lin Xu), the Key project of Cutting-edge Clinical Technology of Jiangsu province (BE2016797 to Lin Xu) and the Innovation Capability Development Project of Jiangsu province (BM2015004 to Lin Xu). Program for Development of Innovative Research Teams [Clinical Research Center, BL2012008]; National Natural Science Foundation of China [81172140, 81272532, 81401873 and 81502071]; Priority Academic Program Development of Jiangsu Higher Education Institutions [JX10231801]; National 973 Basic Research Program of China [2013CB911300, in part]; National Natural Science Foundation of China [81272469 and 81572928]; National Science Foundation of Jiangsu Province [BL2012016]. Funding for open access charge: Program for Development of Innovative Research Teams, by Jiangsu Province Clinical Science and Technology Projects [Clinical Research Center, BL2012008]; National Natural Science Foundation of China [81172140, 81272532, 81401873 and 81502071]; Priority Academic Program Development of Jiangsu Higher Education Institutions [JX10231801]. National Natural Science Foundation of China (81272532 and 81672896), Jiangsu province Clinical science and Technology Project

(Clinical Research Center, BL2012008) and the priority Academic Program Development of Jiangsu High Education Institutions (Public Health and Preventive Medicine, JX10231801).

*Conflict of interest statement.* None declared.

## REFERENCES

- Parkin, D.M., Bray, F., Ferlay, J. and Pisani, P. (2005) Global cancer statistics, 2002. *CA Cancer J. Clin.*, **55**, 74–108.
- Enzinger, P.C. and Mayer, R.J. (2003) Esophageal cancer. *N. Engl. J. Med.*, **349**, 2241–2252.
- Matsushima, K., Isomoto, H., Yamaguchi, N., Inoue, N., Machida, H., Nakayama, T., Hayashi, T., Kunizaki, M., Hidaka, S., Nagayasu, T. *et al.* (2011) MiRNA-205 modulates cellular invasion and migration via regulating zinc finger E-box binding homeobox 2 expression in esophageal squamous cell carcinoma cells. *J. Transl. Med.*, **9**, 30.
- Pohl, H. and Welch, H.G. (2005) The role of overdiagnosis and reclassification in the marked increase of esophageal adenocarcinoma incidence. *J. Natl. Cancer Inst.*, **97**, 142–146.
- Carninci, P., Kasukawa, T., Katayama, S., Gough, J., Frith, M.C., Maeda, N., Oyama, R., Ravasi, T., Lenhard, B., Wells, C. *et al.* (2005) The transcriptional landscape of the mammalian genome. *Science*, **309**, 1559–1563.
- Nagano, T. and Fraser, P. (2011) No-nonsense functions for long noncoding RNAs. *Cell*, **145**, 178–181.
- Ginger, M.R., Shore, A.N., Contreras, A., Rijnkels, M., Miller, J., Gonzalez-Rimbau, M.F. and Rosen, J.M. (2006) A noncoding RNA is a potential marker of cell fate during mammary gland development. *Proc. Natl. Acad. Sci. U.S.A.*, **103**, 5781–5786.
- Rinn, J.L., Kertesz, M., Wang, J.K., Squazzo, S.L., Xu, X., Bruggmann, S.A., Goodnough, L.H., Helms, J.A., Farnham, P.J., Segal, E. *et al.* (2007) Functional demarcation of active and silent chromatin domains in human HOX loci by noncoding RNAs. *Cell*, **129**, 1311–1323.
- Dinger, M.E., Amaral, P.P., Mercer, T.R., Pang, K.C., Bruce, S.J., Gardiner, B.B., Askarian-Amiri, M.E., Ru, K., Solda, G., Simons, C. *et al.* (2008) Long noncoding RNAs in mouse embryonic stem cell pluripotency and differentiation. *Genome Res.*, **18**, 1433–1445.
- Cesana, M., Cacchiarelli, D., Legnini, I., Santini, T., Sthandier, O., Chinappi, M., Tramontano, A. and Bozzoni, I. (2011) A long noncoding RNA controls muscle differentiation by functioning as a competing endogenous RNA. *Cell*, **147**, 358–369.
- Wang, P., Xue, Y., Han, Y., Lin, L., Wu, C., Xu, S., Jiang, Z., Xu, J., Liu, Q. and Cao, X. (2014) The STAT3-binding long noncoding RNA lnc-DC controls human dendritic cell differentiation. *Science*, **344**, 310–313.
- Gupta, R.A., Shah, N., Wang, K.C., Kim, J., Horlings, H.M., Wong, D.J., Tsai, M.C., Hung, T., Argani, P., Rinn, J.L. *et al.* (2010) Long non-coding RNA HOTAIR reprograms chromatin state to promote cancer metastasis. *Nature*, **464**, 1071–1076.
- Yuan, S.X., Yang, F., Yang, Y., Tao, Q.F., Zhang, J., Huang, G., Wang, R.Y., Yang, S., Huo, X.S., Zhang, L. *et al.* (2012) Long noncoding RNA associated with microvascular invasion in hepatocellular carcinoma promotes angiogenesis and serves as a predictor for hepatocellular carcinoma patients' poor recurrence-free survival after hepatectomy. *Hepatology*, **56**, 2231–2241.
- Khaitan, D., Dinger, M.E., Mazar, J., Crawford, J., Smith, M.A., Mattick, J.S. and Perera, R.J. (2011) The melanoma-upregulated long noncoding RNA SPRY4-IT1 modulates apoptosis and invasion. *Cancer Res.*, **71**, 3852–3862.
- Ji, P., Diederichs, S., Wang, W., Boing, S., Metzger, R., Schneider, P.M., Tidow, N., Brandt, B., Buerger, H., Bulk, E. *et al.* (2003) MALAT-1, a novel noncoding RNA, and thymosin beta4 predict metastasis and survival in early-stage non-small cell lung cancer. *Oncogene*, **22**, 8031–8041.
- Tong, Y.S., Wang, X.W., Zhou, X.L., Liu, Z.H., Yang, T.X., Shi, W.H., Xie, H.W., Lv, J., Wu, Q.Q. and Cao, X.F. (2015) Identification of the long non-coding RNA POU3F3 in plasma as a novel biomarker for diagnosis of esophageal squamous cell carcinoma. *Mol. Cancer*, **14**, 3.
- Wei, G., Luo, H., Sun, Y., Li, J., Tian, L., Liu, W., Liu, L., Luo, J., He, J. and Chen, R. (2015) Transcriptome profiling of esophageal squamous

- cell carcinoma reveals a long noncoding RNA acting as a tumor suppressor. *Oncotarget*, **6**, 17065–17080.
18. Li, J., Chen, Z., Tian, L., Zhou, C., He, M.Y., Gao, Y., Wang, S., Zhou, F., Shi, S., Feng, X. *et al.* (2014) LncRNA profile study reveals a three-lncRNA signature associated with the survival of patients with oesophageal squamous cell carcinoma. *Gut*, **63**, 1700–1710.
  19. Chen, F.J., Sun, M., Li, S.Q., Wu, Q.Q., Ji, L., Liu, Z.L., Zhou, G.Z., Cao, G., Jin, L., Xie, H.W. *et al.* (2013) Upregulation of the long non-coding RNA HOTAIR promotes esophageal squamous cell carcinoma metastasis and poor prognosis. *Mol. Carcinog.*, **52**, 908–915.
  20. Mercer, T.R., Dinger, M.E. and Mattick, J.S. (2009) Long non-coding RNAs: insights into functions. *Nat. Rev. Genet.*, **10**, 155–159.
  21. Wilusz, J.E., Sunwoo, H. and Spector, D.L. (2009) Long noncoding RNAs: functional surprises from the RNA world. *Genes Dev.*, **23**, 1494–1504.
  22. Poliseno, L., Salmena, L., Zhang, J., Carver, B., Haveman, W.J. and Pandolfi, P.P. (2010) A coding-independent function of gene and pseudogene mRNAs regulates tumour biology. *Nature*, **465**, 1033–1038.
  23. Nissan, A., Stojadinovic, A., Mitrani-Rosenbaum, S., Halle, D., Grinbaum, R., Roistacher, M., Bochem, A., Dayanc, B.E., Ritter, G., Gomceli, I. *et al.* (2012) Colon cancer associated transcript-1: a novel RNA expressed in malignant and pre-malignant human tissues. *Int. J. Cancer*, **130**, 1598–1606.
  24. Zhu, H., Zhou, X., Chang, X., Li, H., Liu, F., Ma, C. and Lu, J. (2015) CCAT1 promotes hepatocellular carcinoma cell proliferation and invasion. *Int. J. Clin. Exp. Pathol.*, **8**, 5427–5434.
  25. Ma, M.Z., Chu, B.F., Zhang, Y., Weng, M.Z., Qin, Y.Y., Gong, W. and Qian, Z.W. (2015) Long non-coding RNA CCAT1 promotes gallbladder cancer development via negative modulation of miRNA-218-5p. *Cell Death Dis.*, **6**, e1583.
  26. Mizrahi, I., Mazeh, H., Grinbaum, R., Beglaibter, N., Wilschanski, M., Pavlov, V., Adileh, M., Stojadinovic, A., Avital, I., Gure, A.O. *et al.* (2015) Colon cancer associated transcript-1 (CCAT1) Expression in adenocarcinoma of the stomach. *J. Cancer*, **6**, 105–110.
  27. Marchese, F.P. and Huarte, M. (2014) Long non-coding RNAs and chromatin modifiers: their place in the epigenetic code. *Epigenetics*, **9**, 21–26.
  28. Cao, R., Wang, L., Wang, H., Xia, L., Erdjument-Bromage, H., Tempst, P., Jones, R.S. and Zhang, Y. (2002) Role of histone H3 lysine 27 methylation in Polycomb-group silencing. *Science*, **298**, 1039–1043.
  29. Khalil, A.M., Guttman, M., Huarte, M., Garber, M., Raj, A., Rivea Morales, D., Thomas, K., Presser, A., Bernstein, B.E., van Oudenaarden, A. *et al.* (2009) Many human large intergenic noncoding RNAs associate with chromatin-modifying complexes and affect gene expression. *Proc. Natl. Acad. Sci. U.S.A.*, **106**, 11667–11672.
  30. Tsai, M.C., Manor, O., Wan, Y., Mosammamaparast, N., Wang, J.K., Lan, F., Shi, Y., Segal, E. and Chang, H.Y. (2010) Long noncoding RNA as modular scaffold of histone modification complexes. *Science*, **329**, 689–693.
  31. Yoon, J.H., Abdelmohsen, K., Kim, J., Yang, X., Martindale, J.L., Tominaga-Yamanaka, K., White, E.J., Orjalo, A.V., Rinn, J.L., Kreft, S.G. *et al.* (2013) Scaffold function of long non-coding RNA HOTAIR in protein ubiquitination. *Nat. Commun.*, **4**, 2939.
  32. Puvvula, P.K., Desetty, R.D., Pineau, P., Marchio, A., Moon, A., Dejean, A. and Bischof, O. (2014) Long noncoding RNA PANDA and scaffold-attachment-factor SAFA control senescence entry and exit. *Nat. Commun.*, **5**, 5323.
  33. Wang, D., Zhou, J., Liu, X., Lu, D., Shen, C., Du, Y., Wei, F.Z., Song, B., Lu, X., Yu, Y. *et al.* (2013) Methylation of SUV39H1 by SET7/9 results in heterochromatin relaxation and genome instability. *Proc. Natl. Acad. Sci. U.S.A.*, **110**, 5516–5521.
  34. Bennani-Baiti, I.M. (2011) Epigenetic and epigenomic mechanisms shape sarcoma and other mesenchymal tumor pathogenesis. *Epigenomics*, **3**, 715–732.
  35. Vanas, V., Muhlbacher, E., Kral, R. and Sutterluty-Fall, H. (2014) Sprout4 interferes with cell proliferation and migration of breast cancer-derived cell lines. *Tumour Biol.*, **35**, 4447–4456.
  36. Wang, J., Thompson, B., Ren, C., Ittmann, M. and Kwabi-Addo, B. (2006) Sprout4, a suppressor of tumor cell motility, is down regulated by DNA methylation in human prostate cancer. *Prostate*, **66**, 613–624.
  37. Tennis, M.A., Van Scoyk, M.M., Freeman, S.V., Vandervest, K.M., Nemenoff, R.A. and Winn, R.A. (2010) Sprout4 inhibits transformed cell growth, migration and invasion, and epithelial-mesenchymal transition, and is regulated by Wnt7A through PPARGamma in non-small cell lung cancer. *Mol. Cancer Res.*, **8**, 833–843.
  38. Mirabello, L., Kratz, C.P., Savage, S.A. and Greene, M.H. (2012) Promoter methylation of candidate genes associated with familial testicular cancer. *Int. J. Mol. Epidemiol. Genet.*, **3**, 213–227.
  39. Bhatlekar, S., Fields, J.Z. and Boman, B.M. (2014) HOX genes and their role in the development of human cancers. *J. Mol. Med. (Berl)*, **92**, 811–823.
  40. Muckstein, U., Tafer, H., Hackermuller, J., Bernhart, S.H., Stadler, P.F. and Hofacker, I.L. (2006) Thermodynamics of RNA-RNA binding. *Bioinformatics*, **22**, 1177–1182.
  41. Zhang, X.F., Liu, T., Li, Y. and Li, S. (2015) Overexpression of long non-coding RNA CCAT1 is a novel biomarker of poor prognosis in patients with breast cancer. *Int. J. Clin. Pathol.*, **8**, 9440–9445.
  42. He, X., Tan, X., Wang, X., Jin, H., Liu, L., Ma, L., Yu, H. and Fan, Z. (2014) C-Myc-activated long noncoding RNA CCAT1 promotes colon cancer cell proliferation and invasion. *Tumour Biol.*, **35**, 12181–12188.
  43. Yang, F., Xue, X., Bi, J., Zheng, L., Zhi, K., Gu, Y. and Fang, G. (2013) Long noncoding RNA CCAT1, which could be activated by c-Myc, promotes the progression of gastric carcinoma. *J. Cancer Res. Clin. Oncol.*, **139**, 437–445.
  44. Yang, F., Huo, X.S., Yuan, S.X., Zhang, L., Zhou, W.P., Wang, F. and Sun, S.H. (2013) Repression of the long noncoding RNA-LET by histone deacetylase 3 contributes to hypoxia-mediated metastasis. *Mol. Cell*, **49**, 1083–1096.
  45. Zhou, Y., Zhang, X. and Klibanski, A. (2012) MEG3 noncoding RNA: a tumor suppressor. *J. Mol. Endocrinol.*, **48**, R45–53.
  46. Nie, F.Q., Sun, M., Yang, J.S., Xie, M., Xu, T.P., Xia, R., Liu, Y.W., Liu, X.H., Zhang, E.B., Lu, K.H. *et al.* (2015) Long noncoding RNA ANRIL promotes non-small cell lung cancer cell proliferation and inhibits apoptosis by silencing KLF2 and P21 expression. *Mol. Cancer Ther.*, **14**, 268–277.
  47. Sun, M., Liu, X.H., Lu, K.H., Nie, F.Q., Xia, R., Kong, R., Yang, J.S., Xu, T.P., Liu, Y.W., Zou, Y.F. *et al.* (2014) EZH2-mediated epigenetic suppression of long noncoding RNA SPRY4-IT1 promotes NSCLC cell proliferation and metastasis by affecting the epithelial-mesenchymal transition. *Cell Death Dis.*, **5**, e1298.
  48. Xu, T.P., Liu, X.X., Xia, R., Yin, L., Kong, R., Chen, W.M., Huang, M.D. and Shu, Y.Q. (2015) SP1-induced upregulation of the long noncoding RNA TINCR regulates cell proliferation and apoptosis by affecting KLF2 mRNA stability in gastric cancer. *Oncogene*, **34**, 5648–5661.
  49. Zhang, E.B., Kong, R., Yin, D.D., You, L.H., Sun, M., Han, L., Xu, T.P., Xia, R., Yang, J.S., De, W. *et al.* (2014) Long noncoding RNA ANRIL indicates a poor prognosis of gastric cancer and promotes tumor growth by epigenetically silencing of miR-99a/miR-449a. *Oncotarget*, **5**, 2276–2292.
  50. Vire, E., Brenner, C., Deplus, R., Blanchon, L., Fraga, M., Didelot, C., Morey, L., Van Eynde, A., Bernard, D., Vanderwinden, J.M. *et al.* (2006) The Polycomb group protein EZH2 directly controls DNA methylation. *Nature*, **439**, 871–874.
  51. Fahrner, J.A., Eguchi, S., Herman, J.G. and Baylin, S.B. (2002) Dependence of histone modifications and gene expression on DNA hypermethylation in cancer. *Cancer Res.*, **62**, 7213–7218.
  52. Pearson, J.C., Lemons, D. and McGinnis, W. (2005) Modulating Hox gene functions during animal body patterning. *Nat. Rev. Genet.*, **6**, 893–904.
  53. Shah, N. and Sukumar, S. (2010) The Hox genes and their roles in oncogenesis. *Nat. Rev. Cancer*, **10**, 361–371.
  54. Kalinowski, F.C., Brown, R.A., Ganda, C., Giles, K.M., Epis, M.R., Horsham, J. and Leedman, P.J. (2014) microRNA-7: a tumor suppressor miRNA with therapeutic potential. *Int. J. Biochem. Cell Biol.*, **54**, 312–317.
  55. Prensner, J.R., Iyer, M.K., Balbin, O.A., Dhanasekaran, S.M., Cao, Q., Brenner, J.C., Laxman, B., Asangani, I.A., Grasso, C.S., Kominsky, H.D. *et al.* (2011) Transcriptome sequencing across a prostate cancer cohort identifies PCAT-1, an unannotated lincRNA implicated in disease progression. *Nat. Biotechnol.*, **29**, 742–749.